Bull. Mater. Sci., Vol. 34, No. 3, June 2011, pp. 577–581. © Indian Academy of Sciences.

Microwave-assisted synthesis of high-loading, highly dispersed Pt/carbon aerogel catalyst for direct methanol fuel cell

ZHIJUN GUO, HONG ZHU[†,*], XINWEI ZHANG, FANGHUI WANG, YUBAO GUO and YONGSHENG WEI

Department of Chemistry, School of Science, Beijing Jiaotong University, Beijing 100044, China
[†]Institute of Modern Catalyst, State Key Laboratory of Chemical Resource Engineering, School of Science, Beijing University of Chemical Technology, Beijing 100029, China

MS received 26 July 2010; revised 14 September 2010

Abstract. **A Pt supported on carbon aerogel catalyst has been synthesized by the microwave-assisted polyol process. The Pt supported on carbon aerogel catalyst was characterized by high resolution transmission electron microscopy and X-ray diffraction. The results show a uniform dispersion of spherical Pt nanoparticles 2·5–3·0 nm in diameter. Cyclic voltammetry and chronoamperometry were used to evaluate the electrocatalytic activity of the Pt/carbon aerogel catalyst for methanol oxidation at room temperature. The Pt/carbon aerogel catalyst shows higher electrochemical catalytic activity and stability for methanol oxidation than a commercial Pt/C catalyst of the same Pt loading.**

Keywords. **Direct methanol fuel cell; carbon aerogel; Pt; microwave-assisted polyol process; electrocatalyst; electrocatalytic activity.**

1. Introduction

Polymer electrolyte fuel cells, particularly direct methanol fuel cells (DMFCs), are recognized to be a promising electrochemical device. In the last few decades, tremendous effort has been made to develop catalysts for DMFCs (Wasmus and Kuver 1999; Bai *et al* 2006). Despite many efforts and improvements, the commercialization of DMFC is still hindered by several factors, such as low electrocatalytic activity of catalysts for methanol oxidation, high costs of noble metal catalysts, and susceptibility of the catalysts for methanol oxidation reaction. One possibility to enhance the electrocatalytic activity of catalysts and increase the utilization of noble metal catalysts is to increase the surface area of the noble metal by dispersing it on an appropriate support. The importance of the relationship between microstructure and electrocatalytic performance is well recognized. In the past 20 years, several carbon materials such as carbon nanotube, carbon nanofiber, and tungsten carbide were studied as catalyst supports. Recently carbon aerogel (CA) has attracted attention as a new support material for electrocatalysts for fuel cells. Carbon aerogel is a new kind of carbon material (Pekala 1989; Saliger *et al* 1998; Maldonado-Hodar *et al* 1999; Liang *et al* 2000; Wu *et al* 2004). Carbon aerogel possesses high electrical conductivity, high surface area, controllable mesopores, and sharp pore size distribution. The electrocatalytic activity of catalysts is closely related to their preparation method. In recent years, the microwave-assisted heating method has received great attention as a promising method for the preparation of monodispersed nanoparticles. The microwave-assisted heating method is simple, fast, and energy efficient (Chen *et al* 2002; Liu *et al* 2004; Chen *et al* 2004; Tompsett *et al* 2006; Zhu and Zhu 2006; Ma *et al* 2007).

In this study, a simple microwave-assisted polyol process for preparing high-loading, highly dispersed Pt nanoparticles supported on carbon aerogel is reported. The physical and electrochemical properties of the prepared Pt/carbon aerogel (Pt/CA) catalyst were compared with those of the commercial Pt/C catalyst JM (Johnson Matthey).

2. Experimental

2.1 *Preparation*

An organic aerogel was prepared by the sol–gel process from resorcinol and formaldehyde mixtures dissolved in water with sodium carbonate as catalyst. The carbon aerogel was obtained from the carbonization of the dried organic aerogel in a quartz tube furnace at 1050° for 4 hours under a nitrogen atmosphere. Pt/CA catalysts were prepared from the platinum precursor $H_2PtCl_6{\cdot}6H_2O$. In a 100 mL beaker, an ethylene glycol solution of H_2PtCl_6 (10·8 mL, 19·3 mM/L) was mixed with 25 mL of ethylene glycol, followed by 30 minutes of ultrasonic agitation. Then 0·4 mL of 0·4 M

*Author for correspondence (zhuho128@126.com)

KOH solution was added dropwise. Carbon aerogel powder (0·06 g) was uniformly dispersed in the final solution by ultrasonic agitation. The beaker was placed at the centre of a microwave oven (Galanz, 2450 MHz, 800 W) and heated for 180 s (in 6 cycles of 20 s on with 10 s off). The resulting suspension was filtered, and the residue was washed with deionized water and then dried in a vacuum oven at 80°C for 12 hours. The dried residue (0·01 g) was mixed with ethanol (4 mL) and 2·5 wt% Nafion (Aldrich) (0·1 mL) with ultrasonic stirring to form a homogeneous ink. The working electrode was prepared by dropping 10 μL of the ink onto a commercial glassy carbon (GC) disk electrode by a microsyringe and drying at room temperature.

2.2 *Characterization*

X-ray diffraction (XRD) patterns of the Pt/CA catalyst and Pt/C catalyst (JM) were recorded with a powder X-ray diffractometer (Rigaku, D/MAX-RB) using Cu Kà radiation with a Ni filter. The tube current was 40 mA with a tube voltage of 40 kV. The angle was extended from 15 to 85° at a step size of 0·02°. The morphology of the catalyst was characterized by high resolution transmission electron microscopy (HRTEM, JEM-3010). Electrochemical measurements were carried out in a 250 mL three-electrode cell at 25°C with the use of an electrochemistry workstation (CHI 760B). A GC electrode (5 mm in diameter), a Pt-wire electrode, and a saturated calomel electrode (SCE) were used as a working electrode, a counter electrode, and a reference electrode, respectively. All potentials are referenced with respect to the saturated calomel electrode (SCE) in this paper. The cyclic voltammetry (CV) of the catalysts were measured in a potential range of −0·25–1·2 V and at a scan rate of 50 mV/s at 25°C in 0·5 mol/L H_2SO_4 and 0·5 mol/L H_2SO_4+0·5 mol/L CH_3OH solutions. O_2 was removed from the solutions after saturating with high-purity N_2 gas. The chronoamperometry curves were obtained by polarizing the electrode at 0·65 V for 1000 s in the 0·5 mol/L H_2SO_4+0·5 mol/L CH_3OH solution.

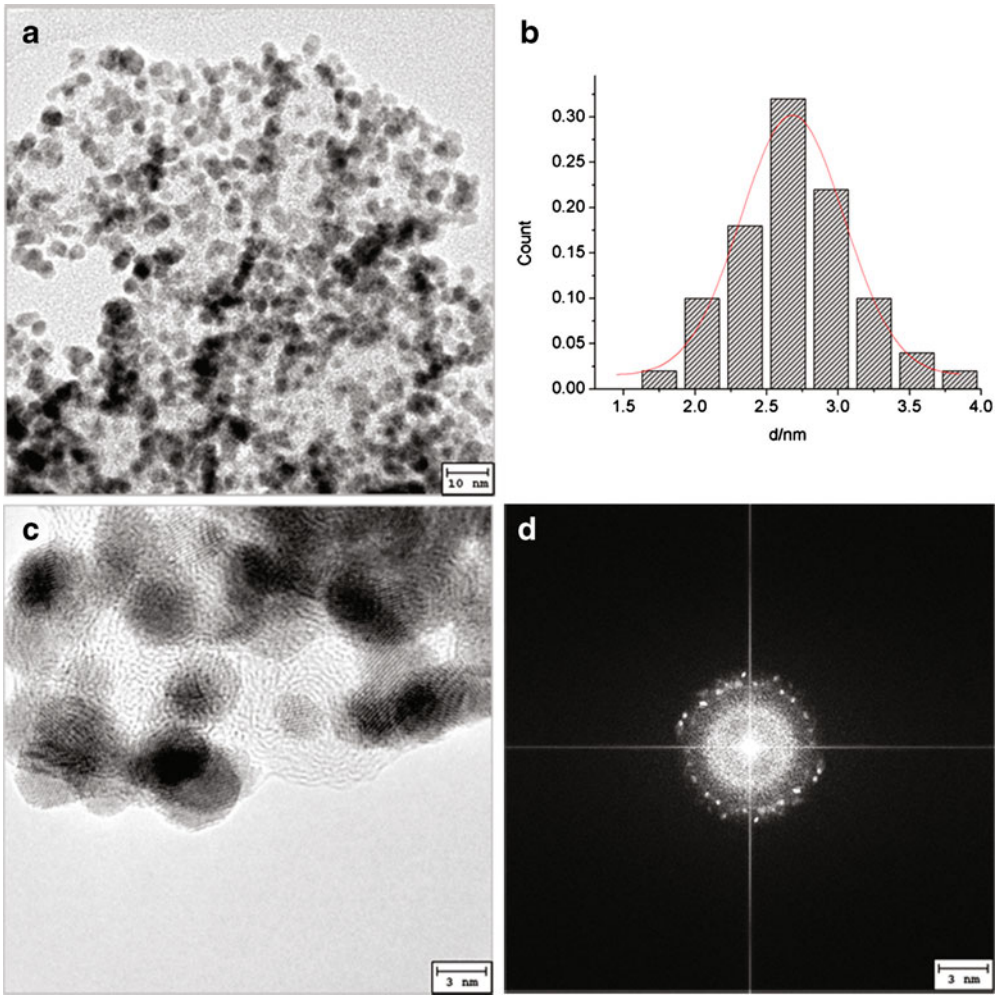

Figure 1. (**a**) and (**c**) HRTEM images; (**b**) histograms of particle size distribution; and (**d**) electron diffraction pattern of a region of Pt/CA catalyst.

3. Results and discussion

Figure 1 shows the HRTEM images (a and c), the corresponding histograms of particle size distribution (b), and the corresponding electron diffraction pattern of a region of the Pt/CA catalyst (d). There is no obvious agglomeration in the sample. Figure 1(a) shows that the platinum–carbon aerogel catalyst consists of well-dispersed spherical platinum particles with an average diameter of 2·70 nm. The histograms of the Pt particle size distribution of the Pt/CA catalyst (figure 1(b)) are obtained based on measurements of over 200 platinum particles.

XRD patterns for Pt/CA and Pt/C catalysts are shown in figure 2. The first weak diffraction peak of [002] reflection indicates the lower degree of graphitization of the reference for carbon aerogel. The characteristic diffraction peaks Pt [111] at 39°, Pt [200] at 45°, Pt [220] at 68°, and Pt [311] at 82° for a face-centred cubic (fcc) structure are observed. The wide diffraction peaks of the catalysts indicate that the particle size of the platinum is very small, as shown in the HRTEM images.

The mean crystallite size of the catalysts was calculated via the Scherrer equation from the Pt [220] diffraction peak after background subtraction. The Scherrer equation is given by Hsin *et al* (2007)

$$d = \frac{0{\cdot}9\lambda_{k\alpha 1}}{B_{(2\theta)}\cos\theta_{\max}}, \tag{1}$$

where d is the average particle size (nm), $\lambda_{k\alpha 1}$ is the wavelength of X-ray radiation (0·1542 nm), $B_{(2\theta)}$ is the width (in radians) of the diffraction peak at half height, and $\theta_{\max}$ is the angle of the diffraction peak [220].

The surface area of platinum (S) is obtained from the average diameter of the particles from HRTEM and XRD results by using the following equation (Guo *et al* 2005)

$$S = \frac{6000}{d\rho}, \tag{2}$$

where S is the surface area (m^2/g), d is the average particle size (nm), and ρ is the density of platinum (21·4 g/cm^3).

The catalysts' mean crystallite size and surface area as obtained from HRTEM and XRD are listed in table 1. The average catalyst particle size calculated from the XRD peak widths agrees well with the HRTEM results.

Table 1. Particle size, specific surface area, and EAS of 40% Pt/CA catalyst and 40% Pt/C catalyst (JM).

	D (nm)		S (m^2/g)		S_{EAS}
Sample	D_{TEM}	D_{XRD}	S_{TEM}	S_{XRD}	(m^2/g)
Pt/CA (40%)	2·70	2·88	103·83	97·35	50·04
Pt/C (40%)	3·30	3·43	84·96	81·74	43·65

To investigate the electrocatalytic activity of the 40 wt.% Pt/CA catalyst, electrochemical measurements were carried out in 0·5 mol/L H_2SO_4 aqueous solution and 0·5 mol/L H_2SO_4 + 0·5 mol/L CH_3OH aqueous solution at 25°C. The cyclic voltammetry curves of the Pt/CA catalyst and Pt/C catalyst (JM) in 0·5 mol/L H_2SO_4 aqueous solution are given in figure 3. The different hydrogen oxidation peaks are due to the presence of different Pt facets in the potential region −0·25 V–0·05 V. The well-defined Pt facets for the hydrogen oxidation peaks observed on the Pt/CA catalyst are similar to those on the commercial Pt/C catalyst (JM) because of the similar graphitic nature of the carbon aerogel and the carbon in the Pt/C catalyst. Pt/CA shows higher current density, indicating that the Pt/CA catalyst has higher electrochemical active area.

The electrochemical active surface (EAS) is calculated from the hydrogen desorption peak area (Q_H) on the cyclic voltammetry curves according to the following equation (Pozio *et al* 2002):

$$S_{EAS} = \frac{Q_H}{0{\cdot}21[Pt]V_{scan}}, \tag{3}$$

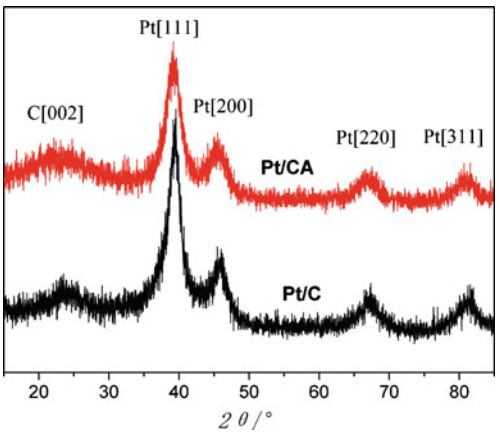

Figure 2. XRD patterns of Pt/CA catalyst and Pt/C catalyst (JM).

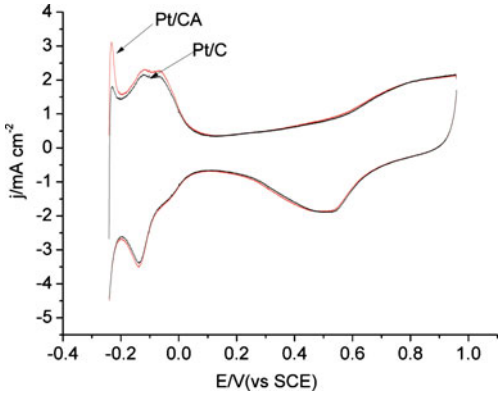

Figure 3. Cyclic voltammetry curves of Pt/CA catalyst and Pt/C catalyst (JM) in 0·5 mol/L H_2SO_4 solution.

where the value of 0·21 (mC/cm^2) represents the charge required to oxidize a monolayer of hydrogen, [Pt] is the platinum loading in the working electrode, and V_{scan} is the scan rate. The EAS data of the Pt/CA catalyst and commercial Pt/C catalyst are given in table 1.

The cyclic voltammetry curves of the Pt/CA, Pt/C and the pure Pt electrode in 0·5 mol/L H_2SO_4 + 0·5 mol/L CH_3OH aqueous solution are presented in figure 4. It can be seen from figure 4 that one peak in the forward scan and one peak in the reverse scan also developed for Pt/CA and Pt/C, showing similar voltammetric characteristics to the pure Pt electrode. However, the methanol oxidation current density increases significantly for Pt/CA and Pt/C compared to the pure Pt electrode. An obvious negative shift of the peak potential can be observed at Pt/CA and Pt/C compared to the pure Pt electrode. This shows that the electrocatalytic effect of methanol is due to Pt nanoparticles. The forward anodic peak between 0·50 V and 0·85 V is due to the oxidation of methanol. In the backward scan, the oxidation peak between 0·20 V and 0·50 V is due to the oxidation of CO or CO-like species that are generated via the incomplete oxidation of methanol in the forward scan. Based on previous publication, the mechanism of methanol oxidation in acid solution can be summarized in the following reactions (Manoharan and Goodenough 1992; Jusys and Behm 2001; Liu *et al* 2010):

$$CH_3OH_{ads} + Pt \rightarrow PtCO_{ads} + 4H^+ + 4e^-,$$

$$H_2O + Pt \rightarrow PtOH_{ads} + H^+ + e^-,$$

$$PtOH_{ads} + PtCO_{ads} \rightarrow Pt + Pt + CO_2 + H^+ + e^-.$$

Although the onset potentials for methanol oxidation on the Pt/CA catalyst and Pt/C catalyst (JM) are almost the same, the peak current density for methanol oxidation of the Pt/CA catalyst is higher than that of the commercial Pt/C catalyst (JM). It should be noted that the peak potential for methanol oxidation of the Pt/CA catalyst shifted 10 mV in the negative direction relative to the commercial Pt/C catalyst (JM). Both results indicate that using carbon aerogel as catalyst support can accelerate the oxidation of methanol due to the high surface area, the active mesoporous structure, and the graphitized structure.

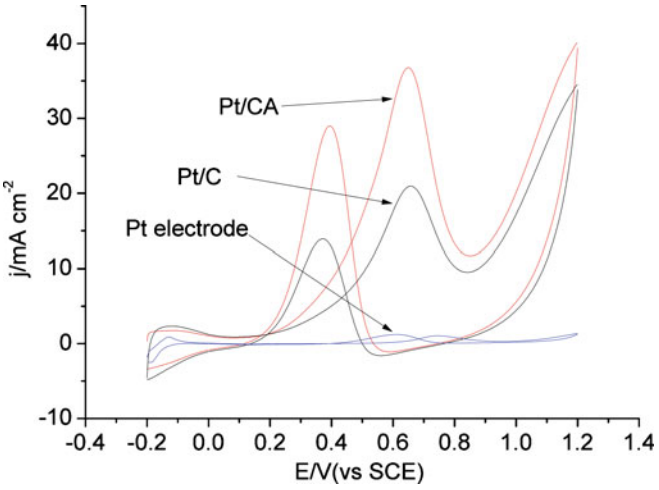

Figure 4. Cyclic voltammetry curves of Pt/CA catalyst, Pt/C catalyst (JM) and the pure Pt electrode in 0·5 mol/L H_2SO_4+0·5 mol/L CH_3OH solution.

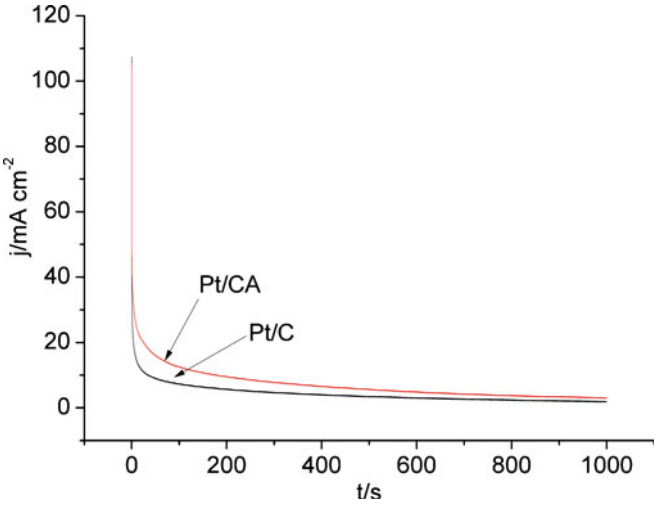

Figure 5. Chronoamperometry curves of Pt/CA catalyst and Pt/C catalyst (JM) in 0·5 mol/L H_2SO_4+0·5 mol/L CH_3OH solution.

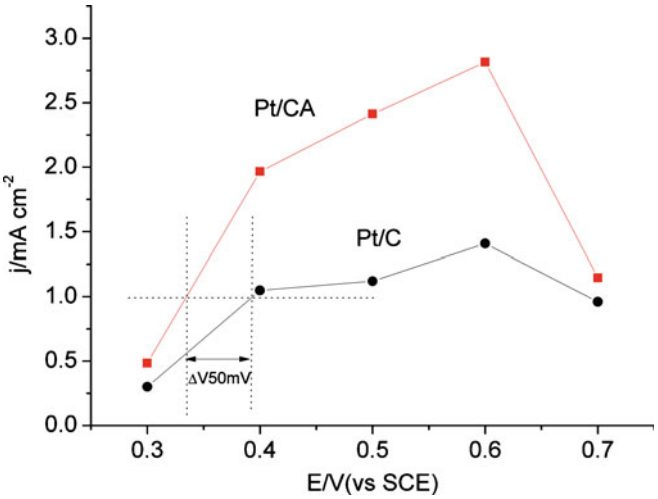

Figure 6. Potential-dependent steady-state current density of methanol oxidation on Pt/CA catalyst and Pt/C catalyst (JM).

Chronoamperometry measurements were made to provide further information on the electrochemical activity and stability of the Pt/CA catalyst for methanol oxidation. Figure 5 shows the current density vs time curves of the Pt/CA catalyst and Pt/C catalyst (JM) at a steady potential of 0·65 V for 1000 s. Similar to the CV results, the Pt/CA catalyst gives a higher limiting current density than the commercial catalyst. This also indicates that the Pt/CA catalyst has higher electrocatalytic activity and stability for methanol oxidation than those of the Pt/C catalyst (JM) at the same Pt loading (40%).

The enhanced electrochemical properties of the Pt/CA catalyst are due to the formation of smaller Pt nanoparticles and the excellent characteristics of the carbon aerogel.

The steady-state current density obtained from chronoamperometry measurements (recorded for various potentials, 0·3 V to 0·7 V) corresponding to methanol oxidation is plotted against each respective potential in figure 6 in order to compare current density (Mahima *et al* 2008; Subhramannia *et al* 2008). The current density on Pt/CA form 0·3 V to 0·7 V is higher than that on Pt/C. Pt/CA and Pt/C electrodes show maximum activity at a potential of 0·6 V. From the potential-dependent current density curve, it is obvious that the potential on Pt/CA is shifted negatively by 50 mv as compared to that of Pt/C at the same current density of 1·0 mA/cm^2. Hence, the Pt/CA catalyst exhibits higher catalytic activity for the oxidation of methanol than Pt/C catalyst.

All the electrochemical test results show that the platinum/carbon aerogel is a good catalyst for methanol oxidation and carbon aerogel is a good catalyst support for fuel cells.

4. Conclusions

A high-loading and highly dispersed 40 wt% platinum/carbon aerogel catalyst has been synthesized by the microwave-heated polyol method. The morphological properties of the platinum/carbon aerogel catalyst are evaluated by HRTEM, and it is found that the Pt particles have been well dispersed on the carbon aerogel with a mean size of 2·70 nm. XRD analyses show the formation of Pt in the fcc phase. The average size of the platinum nanoparticles calculated from the XRD data agree well with the HRTEM results. The cyclic voltammetry curves in 0·5 mol/L H_2SO_4 aqueous solution show that the Pt/CA catalyst has a higher electrocatalytic surface area than that of a commercial Pt/C catalyst (JM) under the same Pt loading. The results from cyclic voltammetry and chronoamperometry measurements indicate that the Pt/CA catalyst shows higher electrochemical catalytic activity and electrochemical stability for methanol oxidation compared with the commercial catalyst. Based on all the results, we conclude that the Pt/CA catalyst has considerable potential to be an electrocatalyst for direct methanol fuel cells.

Acknowledgements

The authors gratefully acknowledge the financial support from the National Science Foundation of China (No. 20876013 and Key Program No. 20636060) and International S&T Cooperation Program of China (No. 2009DFA63120).

References

Bai Y, Wu D, Wu F and Yi B L 2006 *Mater. Lett.* **60** 2236
Chen W X, Lee J Y and Liu Z L 2002 *Chem. Commun.* **21** 2588
Chen W X, Lee J Y and Liu Z L 2004 *Mater. Lett.* **58** 3166
Guo J W, Zhao T S, Prabhuram J and Wong C W 2005 *Electrochim. Acta* **50** 1973
Hsin Y L, Hwang K C and Yeh C T 2007 *J. Am. Chem. Soc.* **129** 9999
Jusys Z and Behm R J 2001 *J. Phys. Chem. B* **105** 10874
Liang C H, Sha G Y and Guo S C 2000 *J. Non-Cryst. Solids* **271** 167
Liu Z L, Lee J Y, Chen W X, Han M and Gan L M 2004 *Langmuir* **20** 181
Liu H J, Wang X M, Cui W J, Dou Y Q, Zhao D Y and Xia Y Y 2010 *J. Mater. Chem.* **20** 4223
Mahima S, Kannan R, Komath I, Aslam M and Pillai V K 2008 *Chem. Mater.* **20** 601
Maldonado-Hodar F J, Ferro-Garcia M A, Rivera-Utrilla J and Moreno-Castilla C 1999 *Carbon* **37** 1199
Ma L, Zhang H M, Liang Y M, Xu D Y, Ye W, Zhang J L and Yi B L 2007 *Catal. Commun.* **8** 921
Manoharan R and Goodenough J B 1992 *J. Mater. Chem.* **2** 875
Pekala R W 1989 *USA Patent* 4873218
Pozio A, Francesco M D, Cemmi A, Cardellini F and Giorgi L 2002 *J. Power Sources* **105** 13
Saliger R, Fischer U, Herta C and Fricke J 1998 *J. Non-Cryst. Solids* **225** 81
Subhramannia M, Ramaiyan K and Pillai V K 2008 *Langmuir* **24** 3576
Tompsett G A, Conner W C and Yngvesson K S 2006 *Chem. Phys. Chem.* **7** 296
Wasmus S and Kuver J 1999 *Electroanal. Chem.* **461** 14
Wu D C, Fu R W, Zhang S, Dresselhaus M S and Dresselhaus G 2004 *Carbon* **42** 2033
Zhu J F and Zhu Y J 2006 *J. Phys. Chem. B* **110** 8593